ISSN 1330–0008
CODEN FIZAE4

TEMPERATURE DISTRIBUTION MEASUREMENT IN AN AXIALLY SYMMETRIC SOURCE WHICH IS NOT OPTICALLY THIN

HRVOJE SKENDEROVIĆ, VLADIS VUJNOVIĆ, NAZIF DEMOLI and JADRANKA RUKAVINA*

Institute of Physics of the University, Bijenička c. 46, Zagreb, Croatia
**Lamp factory, Zagreb*

Received 3 October 1994

UDC 533.95

PACS 35.80.+s

We elaborated two spectroscopic methods for the temperature distribution in axially symmetric source. One method uses the self-reversed spectral line; this method is based on a comparison of the measured absolute maximum (peak) intensity with that calculated as a function of axial temperature. Another method which uses a spectral line without self-reversal, was based on the Kirchhoff's law and exploits two-path absorption technique and Abel transformation. For both methods, knowledge of atomic broadening constants and transition probabilities is not crucial.

1. Introduction

There are several methods of spectroscopic temperature measurements in a gas discharge of cylindrical symmetry, when a plasma is in the local thermal equilibrium [1-3]. In our study, the diagnostics of temperature was applied for a medium which has a wide range of optical depths. Some of the spectral lines show self-reversal, and the others suffer from absorption but do not show self-reversal. The deviation from optical thinness opens additional possibilities for the diagnostics, as well as for the determination of the atomic parameters.

The peak intensity of the self-reversed line is governed by the maximal temperature along the line of sight. We studied the possibility to determine the temperature by synthesizing the complete line profile with the help of transfer of radiation and effective broadening mechanisms. The normalized line profiles used in our calculations, represented by the convolution of the Lorentz and van der Waals quasi-static profiles, are position dependent.

The spectral line without the self-reversal can be suitable for the temperature determination by exploiting the Kirchhoff's law, that means by simultaneous determination of the emission and absorption coefficients. In order to measure the absorption coefficient with reasonable accuracy, the line should have an optical depth within some range of values, say between 0.1 and 0.8.

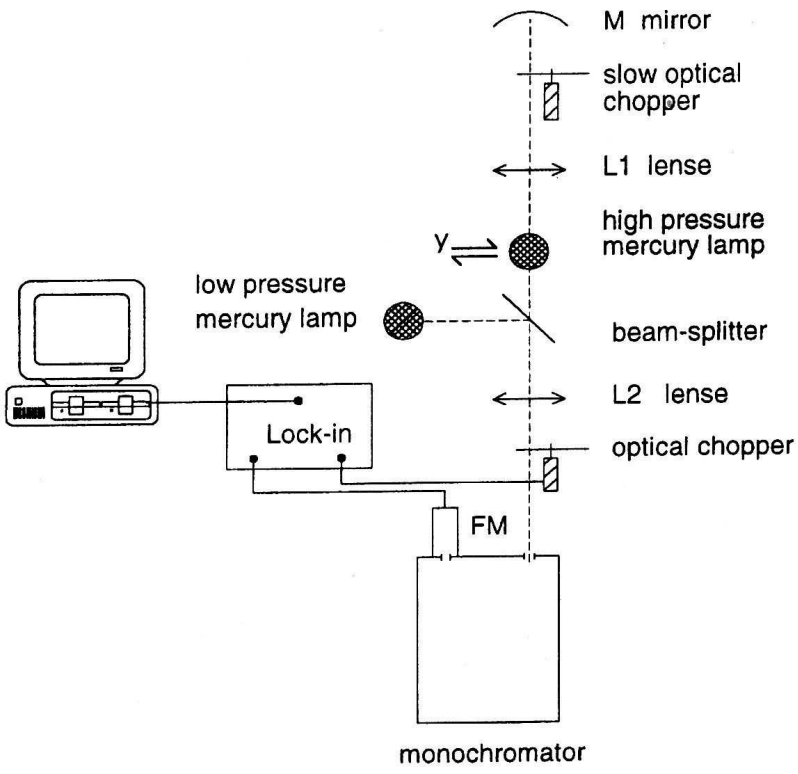

Fig.1. Experimental setup.

The experiment was suited to the requirements (Fig. 1). The source of radiation was a high pressure mercury lamp with the discharge closed in a quartz vessel. The interelectrode distance was 5 cm and the inner radius of the quartz vessel was measured to be 7.8 mm. The discharge was operated on DC current of 2.9 A and the voltage drop on the lamp was 120 V.

Measurement of the absorption coefficient was made possible by the two-path absorption technique [4], as shown in Fig. 1. A concave mirror M was placed at the opposite side of the plasma to the monochromator in order to reflect the image of the plasma on the entrance slit.

A 1.5 m Jobin Yvon THR monochromator was used with the experimentally determined FWHM of instrumental profile of 2.5 pm with the slit widths set at 15 μm. The optical system was aligned using a He-Ne laser beam. The low pressure mercury lamp was used for the wavelength calibration.

The high pressure mercury lamp was mounted on a micrometer screw and allowed to move in the y direction, i. e. the direction perpendicular to the optical axis. Profiles were taken at different lateral positions. Acquisition and processing of the experimental data was carried out by a lock-in amplifier and PC. The intensity signal was calibrated with a tungsten strip-lamp. The error in absolute intensity measurements was evaluated from the tungsten strip-lamp measurements for different currents, and was found to be 3% , the relative intensity error was 1%.

2. *Radiation transfer in the axially symmetric source and a solution for the local absorption coefficient*

The radiance emitted along the line-of-sight placed at a distance y from the axes of symmetry $I_\lambda(y)$ is given by:

$$I_\lambda(y) = \int_{-\sqrt{R^2-y^2}}^{\sqrt{R^2-y^2}} \epsilon_\lambda(r') \exp\left[- \int_{\sqrt{r'^2-y^2}}^{\sqrt{R^2-y^2}} k(\lambda, r'')\, \mathrm{d}x'' \right] \mathrm{d}x' \tag{1}$$

where $\epsilon_\lambda(r')$ is the spectral emission coefficient (power density), $k(\lambda, r'')$ is the absorption coefficient, $r'^2 = y^2 + x'^2$, and $r''^2 = y^2 + x''^2$. In this case, an analogous expression to the Abel transform and its inverse form can be obtained by using the plasma transmission $\omega(\lambda, y)$. The transmission is determined experimentally with a mirror which images the source on itself [4] (Fig. 2).

If the plasma radiance is $I_\lambda(y)$, the direct ray contributes $\tau_1 I_\lambda(y)$. The same radiance is reflected from the mirror and is then absorbed in the source, giving the contribution:

$$I'_\lambda(y) = \tau_1 \tau_2^2 \rho I_\lambda(y) \exp\left[-2 \int_0^{\sqrt{R^2-y^2}} k(\lambda, r')\, \mathrm{d}x' \right] \tag{2}$$

where ρ is the mirror reflectivity. (Transparencies of the frontal and rear wall, τ_1

and τ_2 can be different due to wall structure or turbidity.) The observed radiance is the sum:

$$I_{\lambda M}(y) = \tau_1 I_\lambda(y) \left\{ 1 + \tau_2^2 \rho \cdot \exp \left[-2 \int_0^{\sqrt{R^2-y^2}} k(\lambda, r') \, \mathrm{d}x' \right] \right\} \tag{3}$$

Transmission $\omega(\lambda, y)$ is given by:

$$\omega(\lambda, y) \equiv \frac{I_{\lambda M}(y) - I_\lambda(y)}{R_M I_\lambda(y)} = \exp \left[-2 \int_0^{\sqrt{R^2-y^2}} k(\lambda, r') \, \mathrm{d}x' \right] \tag{4}$$

with the abbreviation $R_M = \tau_2^2 \rho$ having the meaning of an effective mirror reflectivity. R_M is obtained experimentally when comparing single and double path signals on the far wings of the spectral lines where the total optical thickness is negligible. In principle, it depends on the transversal distance y and on the wavelength.

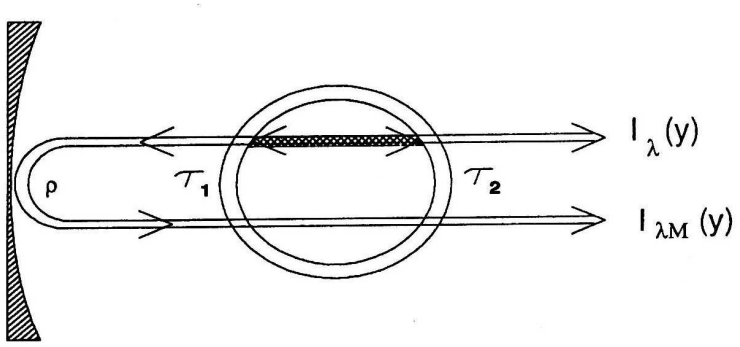

Fig. 2. Double-path absorption technique.

The solution for the absorption coefficient is given by the inverse Abel transform of the transmission:

$$k(\lambda, r) = \frac{1}{\pi} \int_r^R \frac{\mathrm{d}}{\mathrm{d}y} \{ \ln [\omega(\lambda, r)] \} \frac{\mathrm{d}y}{\sqrt{y^2 - r^2}}. \tag{5}$$

The absorption coefficient derived in this way gives all information on the line profile formation. However, precision of the obtained figures is satisfying when the transmission is in the range of between 10% and 80% [5].

When the absorption coefficient is determined, the radiative transfer equation (5) for the double path, rearranged in the following way,

$$\frac{I_\lambda(y)}{\sqrt{\omega(\lambda,y)}} = 2\int_r^R \epsilon_\lambda(r)\cosh\left[G(\lambda,y,r)\right]\frac{r}{\sqrt{r^2-y^2}}\mathrm{d}r, \tag{6}$$

where

$$G(\lambda,y,r) = \int_y^r \frac{k(\lambda,r')}{\sqrt{r'^2-x^2}}\mathrm{d}r' \tag{7}$$

gives possibility to find the emission coefficient by an iterative procedure (see Ref. 5). Numerical solution of the Abel transform has been performed by many investigators. We have taken over the Fourier method from Ref. 6. It avoids derivation and necessity for smoothing the experimental curve.

The absorption measurement technique described above can not be applied to the lines that exhibit self-reversal minimum in the line centre.

3. Synthesis of the self-reversed line profile

In order to synthesize the line shape $I_\lambda(r)$, an essential step is the choice of the normalized position dependent line profile $P(\Delta\lambda, r)$, where $\Delta\lambda = \lambda - \lambda_0$, and where λ_0 is the centre of the line. The line profile $P(\Delta\lambda, r)$ is the same for absorption and emission in the presence of LTE.

For high pressure mercury discharge, with a pressure of several bars, the main broadening mechanism is the pressure broadening. The pressure broadening consists of the broadening by neutral mercury atoms and the broadening by the mercury ions and electrons (Stark broadening). The mechanism of pressure broadening in the line centre differs from the broadening in the line wings. For the broadening in the line centre one usually uses Lorentz profile, $P_1(\Delta\lambda, r)$ and for the wing broadening quasistatic van der Waals profile $P_2(\Delta\lambda, r)$. These profiles are given by [7,8]:

$$P_1(\Delta\lambda, r) = \frac{\Delta\lambda_{1/2}(r)}{\pi}\frac{1}{\Delta\lambda^2 + \Delta\lambda_{1/2}(r)^2}, \tag{8}$$

$$P_2(\Delta\lambda, r) = \frac{\sqrt{\Delta\lambda_0(r)}}{2\Delta\lambda^{3/2}}\exp\left(-\frac{\pi\Delta\lambda_0(r)}{4\Delta\lambda}\right). \tag{9}$$

The Lorentz profile is composed of two contributions, one corresponding to the broadening by the neutral atoms and the other corresponding to the Stark

broadening: $\Delta\lambda_{1/2}(r) = CN(r) + C_S N_e(r)$. The characteristic width of the van der Waals quasistatic profile $\Delta\lambda_0(r)$ is proportional to the square of the atom number density: $\Delta\lambda_0(r) = C_W N(r)^2$.

The total line profile can be approximated by a convolution of these two profiles [9]. The blue wing of the convolved profile behaves like the Lorentzian wing and the red wing like the quasistatic van der Waals wing. The profile $P_2(\Delta\lambda, r)$ contributes very little to the centre of the line where quasistatic approximation fails, if $\Delta\lambda_0$ is smaller than $\Delta\lambda_{1/2}$. The convolution can be solved analytically [9] and is given by:

$$P(\Delta\lambda, r) = \frac{1}{\pi\Delta\lambda_{1/2}(1+a^2)} - \frac{\mathrm{i}c\pi}{2} e^{-ab\,/(1+a^2)} W(a,b), \tag{10}$$

where $W(a,b)$ equals:

$$W(a,b) = Z_1^{3/2} e^{-\mathrm{i}b\,/(1+a^2)} \mathrm{erfc}(\sqrt{Z_1 b}) - Z_2^{3/2} e^{\mathrm{i}b\,/(1+a^2)} \mathrm{erfc}(\sqrt{Z_2 b}), \tag{11}$$

and a, b, c, Z_1 and Z_2 are given by:

$$Z_{1,2} = \frac{-a \mp \mathrm{i}}{1+a^2},$$

$$a = \frac{\Delta\lambda}{\Delta\lambda_{1/2}(r)}, \quad b = \frac{\pi\Delta\lambda_0(r)}{4\Delta\lambda_{1,2}(r)},$$

$$c = \frac{\sqrt{\Delta\lambda_0(r)}}{2\pi[\Delta\lambda(r)_{1/2}]^{3/2}}.$$

We have used rational approximation of the complex error function, $w(z)$, introduced by Fadeyeva and Terent'ev [10], and its connection to the complementary error function $\mathrm{erfc}(z)$ in the complex region. The sixth degree rational approximation to $w(z)$ is given in Ref. 11.

The expressions for $\epsilon_\lambda(r)$ and $k(\lambda, r)$ in LTE were used [12]. Transition probability was taken from Ref. 13. The connection between temperature and number densities is given by the equation of state and Saha equation. Radial temperature distribution was taken as follows:

$$T(r) = T(0) - [T(0) - T(R)] \left(\frac{r}{R}\right)^q \tag{12}$$

with q being a distribution parameter, r the radial distance and R the tube radius. The wall temperature influence is very small in the range from 800-1200 K and

we kept it $T(R) = 1000$ K. Pyrometric measurements [14] performed on similar discharge revealed the wall temperature from 900–1000 K.

Substituting all equations in expression (1), $I_\lambda(y)$ was numerically calculated for the line 546.1 nm. Then, the shapes $I_\lambda(y)$ were convolved with the instrumental profile, and compared with the experimentally obtained ones. We have constructed a set of line shapes varying the following parameters: pressure p, axial temperature $T(0)$, temperature profile parameter q, and constants of proportionality C_N and C_W. The Stark broadening was of minor influence so the value of C_S was taken from Ref. 3.

The profile of the self–reversed spectral line shows a minimum at the unshifted wavelength and two maxima. The maxima are of equal intensity in our calculation. The red maximum is displaced little further than blue one, and the profile is asymmetric showing an extended red wing – all being consequence of the unilateral quasi-static van der Waals broadening.

The spectral line profile is influenced by the parameter q primarily at the self-reversed minimum (Fig. 3). This is the consequence of the temperature distribution. Increasing q, the distribution becomes broad and flat-topped, with a sharp fall at the outskirts. Thus the central high temperature and a low density core is surrounded by the cool and high density envelope.

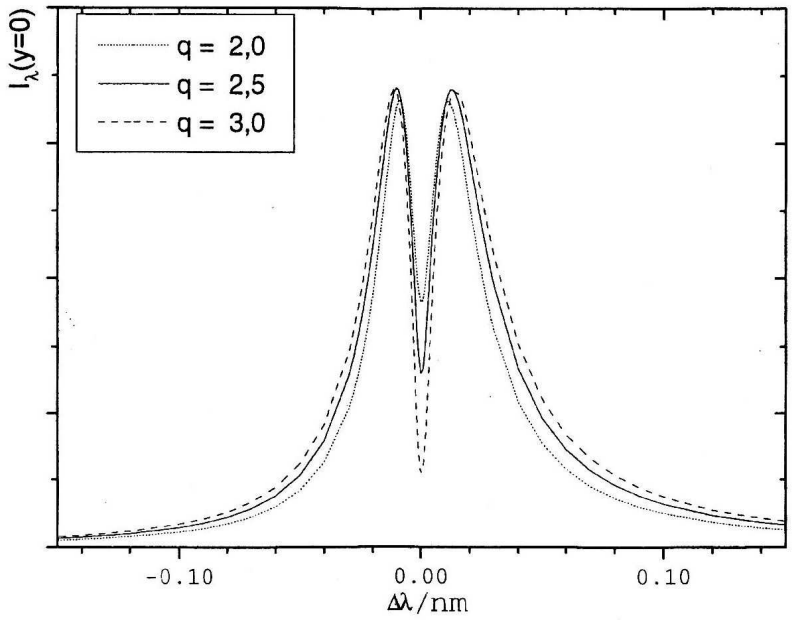

Fig. 3. Influence of the temperature distribution parameter q on the line intensity profile of the line 546.1 nm*: displacement* $y = 0$, *pressure* 3×10^5 Pa, $T(0) = 5700$ K, $C_N = 0.6 \times 10^{-36}$ m^4, $C_S = 0,\ 0.3 \times 10^{-62}$ m^7, $q = 2,\ 2.5,\ 3$.

The increase of the axis temperature with the wall temperature fixed at 1000 K leads to an increase of the temperature at any point in the cross-section. Thus intensity $I_\lambda(y)$ rises noticeable (Fig. 4). The increase of the pressure leads to an increase of the peak separation, at the same time leaving the peak intensities intact (Fig. 5).

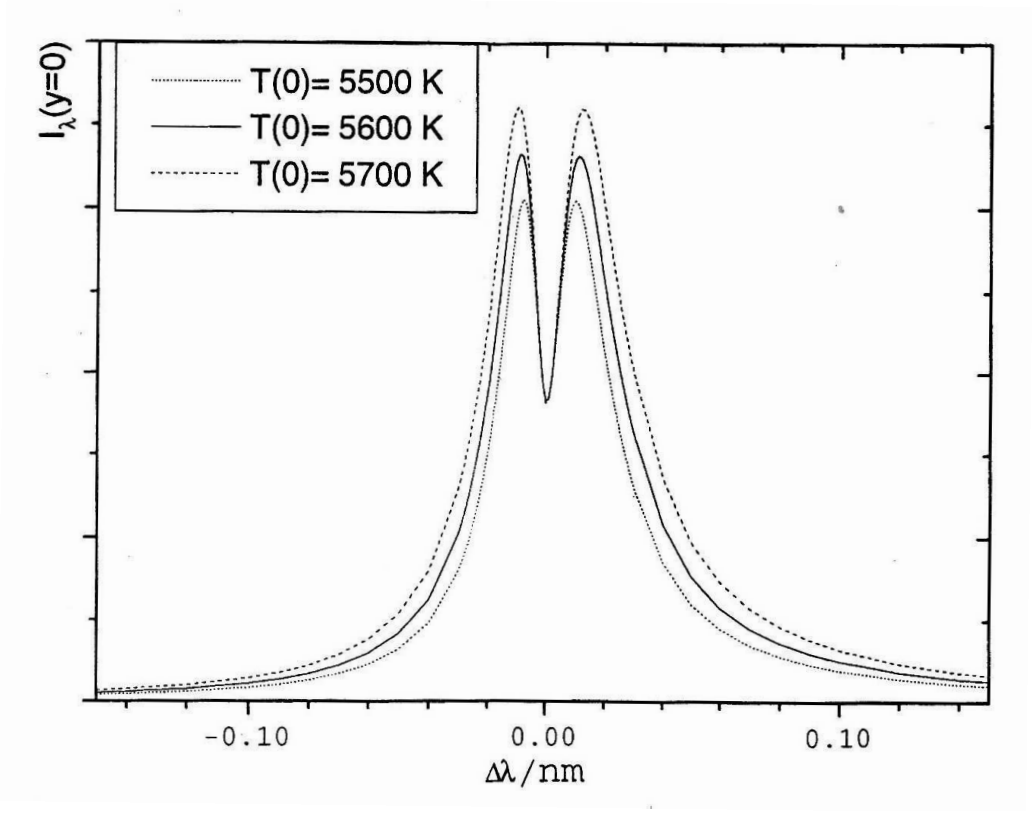

Fig. 4. Influence of the axis temperature $T(0)$ on the line intensity profile of the line 546.1 nm*: $q = 2$, $T(0) = 5500, 5600$ and* 5700 K*. The other parameters are the same as in Fig. 3.*

It was found that the atomic parameters influence the line profile in a more subtle manner. Increase of the broadening constant C_N is followed by a perceptible broadening of wings and filling of the central minimum. Van der Waals broadening has effect only on the red wing. The transition probability has no effect on the peak intensities.

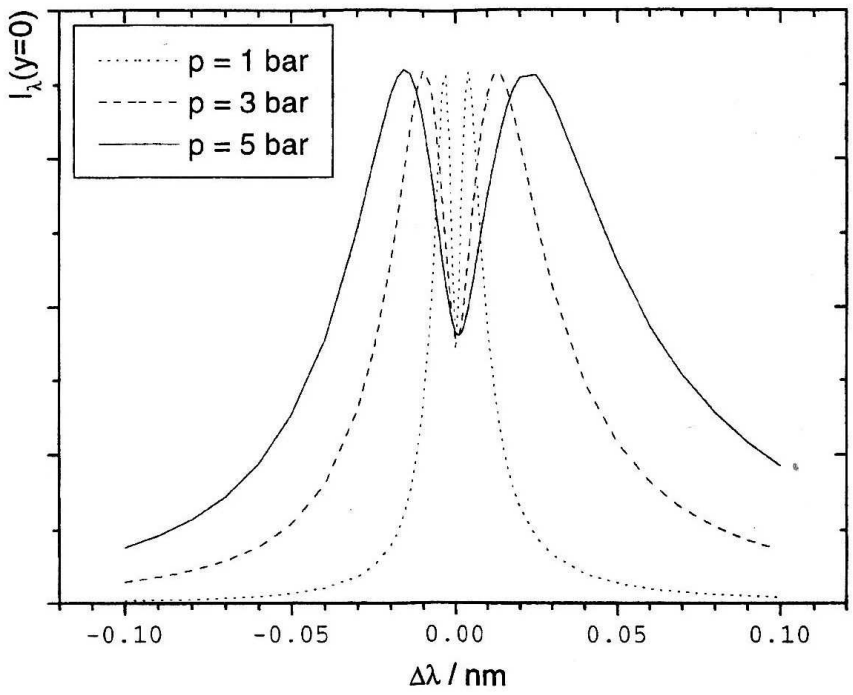

Fig. 5. Influence of the pressure on the line intensity profile of the line 546.1 nm*:* $q = 2$, $p = 10^5,\ 3 \times 10^5,\ 5 \times 10^5$ Pa. *The other parameters are the same as in Fig. 3.*

4. *Temperature determination*

4.1. *Using self-reversed line 546.1* nm

As seen in Section 3, a very strong dependence of the maximum intensity on axis temperature, a weak dependence on the temperature profile parameter q, and no dependence upon the other parameters (pressure, broadening constants, and transition probability) are important prerequisites for the temperature determination. The intensities of the maxima as a function of the axis temperature for different parameters q were plotted for the self-reversed line 546.1 nm in Fig. 6. We have also measured line intensities $I_\lambda(y)$ of the same line for different values of the displacement y.

We have determined the temperature parameter q and the axis temperature $T(0)$ by the following iterative procedure. Firstly, a value of q_0, was picked and from the curve from Fig. 6 for q_0 and from the measured $I_{\lambda MAX}(y = 0)$ the starting axis temperature $T_0(0)$ was determined. With the starting value q_0 the intensity maxima versus temperature $T(0)$ were plotted for the other displacements $y =$

$0.1R, ..., 0.5R$. From these plots the set of $q_1(y)$ values for different y was obtained using Eq. (12) and the average q_1 was calculated. Using the average q_1, the curve $I_{\lambda MAX}(y)$ versus $T(0)$ was plotted. A value for $T_1(0)$ is graphically determined from that curve and the measured $I_{\lambda MAX}(y = 0)$. The iterative procedure terminates when the difference between $T_n(0)$ and $T_{n-1}(0)$ is within reasonable margin of error.

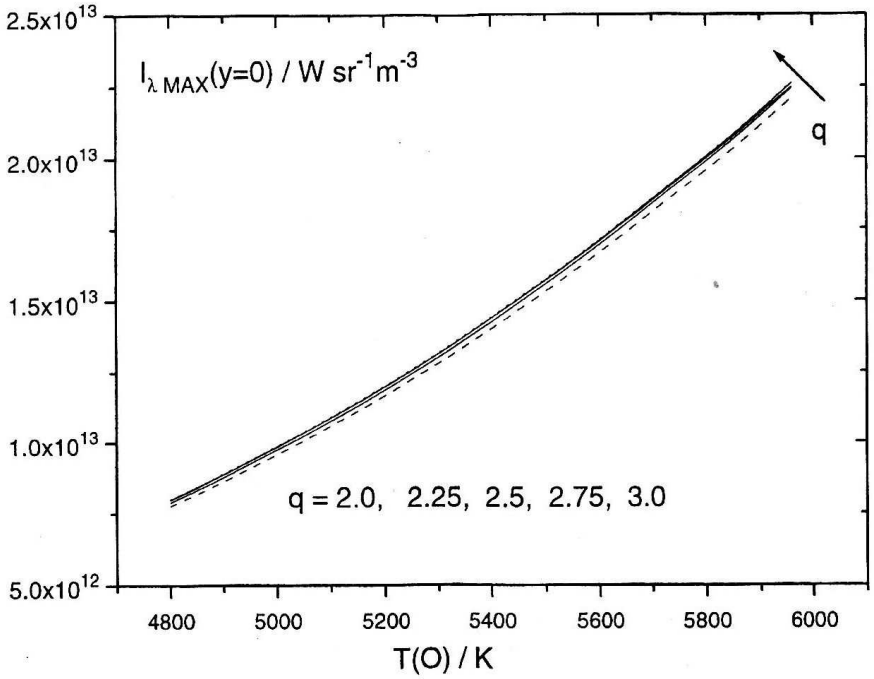

Fig. 6. Dependence of maximum intensity of the spectral line 546.1 nm *on the axis temperature* $T(0)$ *for the position* $y = 0$ *with parameter* $q = 2.0,\ 2.25,\ 2.50,\ 2.75$ *and* 3.0.

The obtained results are $T(0) = (5615 \pm 35)$K, and $q = 2.65$. The temperature error follows from the error in absolute intensity.

4.2. Using line 577.0 nm *that is not self-reversed*

The lower energy level of the transition producing line 577.0 nm is relatively high above ground level, and the maximum optical thickness (i. e. in the centre of the line and for displacement $y = 0$) was equal 0.33 in our case. That makes this line a good candidate for the determination of absorption coefficients by the procedure described in Section 2. After obtaining absorption and spectral emission coefficient the temperature can be calculated from the well-known Kirchhoff's formula that is valid in LTE:

$$B_\lambda(T) = \frac{\epsilon_\lambda(r)}{k(r,\lambda)} \tag{13}$$

where $B_\lambda(T)$ is the black-body radiation of temperature T.

Both intensities with and without the mirror from the line 576.9 nm were measured for different positions y. The spectral emission coefficient $\epsilon_\lambda(r)$ was obtained as Abel transform of the quantity $I_\lambda(y)/\sqrt{\omega(\lambda,y)}$, i. e., the first approximation to the equation (6). Abel transform of the quantity $-\ln[\omega(\lambda,y)]$ leads to the absorption coefficient $k(\lambda,r)$.

The temperature obtained by this line amounts to $T(0) = (5695 \pm 120)$K. The error of temperature determined in this way was evaluated as:

$$\Delta T(r) = \left(\left| \frac{\Delta k(\lambda,r)}{k(\lambda,r)} \right| + \left| \frac{\Delta \epsilon_\lambda(r)}{\epsilon_\lambda(r)} \right| \right) \frac{B_\lambda(T)}{|\partial B_\lambda(T)/\partial T|}. \tag{14}$$

The error $\Delta\epsilon_\lambda(r)$ originates from the error in determination of absolute intensity $I_\lambda(r)$, while the error of absorption coefficient is linked to the error of transmission $\Delta\omega(\lambda,y)$ and was evaluated as:

$$\Delta k(\lambda,r) = \frac{1}{\pi} \int_r^R \frac{\mathrm{d}}{\mathrm{d}y} \left(\frac{\Delta\omega(\lambda,y)}{\omega(\lambda,y)} \right) \frac{\mathrm{d}y}{\sqrt{y^2 - r^2}}. \tag{15}$$

The $\Delta\omega(\lambda,y)$ originates from the relative error in measured intensity.

5. *Conclusion*

The Table 1 compares temperatures obtained using the self-reversed line and using the line that is not self reversed. The temperature was also determined by Bartels' method that uses maximum intensity of the self-reversed line. Since Bartels' method presumes parabolic radial temperature distribution ($q = 2$), de Groot and Jack improved [15] the method allowing for cubic profile ($q = 3$).

TABLE 1.
Axis temperature obtained by different methods: a) using self-reversed line 546.1 nm, *b) using line that is not self-reversed* 577 nm, *c) using Bartels' method ($q = 2$), d) using Bartels' method ($q = 3$).*

	a	b	c	d
$T(0)$	5615 ± 35	5695 ± 120	5593	5571

The Bartels method is of approximate nature. Our more elaborated procedure gives the temperature and parameter q simultaneously. Our result for q (equal to 2.65), shows that the distribution is intermediate between parabolic and cubic, and should be established for each particular discharge. We have proved that convolution of the Lorentz and quasi-static van der Waals profiles that are dependent on the radial position (i.e. have half half-width dependent on temperature and concentration), is realistic since the calculated self-reversed profile closely matches the observed one [16]. For this purpose also, no previous pressure determination was necessary, unlike the procedure described in Ref. 2.

References

1) L. Bober and R. S.Tankin, JQSRT **9** (1969) 855;
2) H. P. Stormberg and R. Schaefer, JQSRT **33** (1985) 27;
3) J. J. Damelincourt, D. Karabourniotis, L. Scoarnec and P. Herbert, J. Phys. D: Appl. Phys. **11** (1978) 1029;
4) P. J. Dickerman and R. W. Deuel, Rev. Sci. Instr. **35** (1964) 978;
5) P. Elder, T. Jerrick and W. Birkeland, Appl. Opt. **4** (1965) 589;
6) G. Pretzler, Z. Naturforsch. **46a** (1991) 639;
7) G. Traving, *Interpretation of line broadening and line shift,* in *Plasma Diagnostics*, ed. W. Lochte-Holtgreven, Amsterdam, North-Holland (1968) 66;
8) H. Margenau, Phys. Rev **48** (1935) 755;
9) H. P. Stormberg, J. Appl. Phys. **51** (1980) 1963;
10) V. N. Fadeyeva and N. M. Terent'ev, *Tables of the Probability Integral for Complex Argument*, Pergamon Press, Oxford (1961);
11) A. K. Hui, B. H. Armstrong and A. A. Wray, JQSRT **19** (1978);
12) R. Richter, *Radiation of hot gases*, in *Plasma Diagnostics*, ed. W. Lochte-Holtgreven, Amsterdam, North-Holland (1968) 214;
13) E. C. Benck, J. E. Lawler and Dakin, J. Opt. Soc. Am. B **6** (1989) 11;
14) D. Karabourniotis, C. Karras, M. Drakakis and J. J. Damelincourt, J. Appl. Phys 53 **11** (1982) 7259;
15) J. J. de Groot and J. Jack, JQSRT **13** (1973) 615;
16) H. Skenderović, M. Sc. thesis, Zagreb (1994).

MJERENJE TEMPERATURNE RASPODJELE U OSNO-SIMETRIČNOM IZVORU KOJI NIJE OPTIČKI TANAK

HRVOJE SKENDEROVIĆ, VLADIS VUJNOVIĆ, NAZIF DEMOLI i JADRANKA RUKAVINA*

Institut za fiziku Sveučilišta, Bijenička cesta 46, Zagreb, Hrvatska
** Tvornica žarulja, Zagreb, Hrvatska*

UDK 533.95

PACS 35.80.+s

Razvili smo spektroskopsku metodu za mjerenje temperaturne raspodjele u osno-simetričnom izvoru. Jedan postupak koristi reverziranu spektralnu liniju; uspoređuje se mjereni apsolutni intenzitet vrhova spektralne linije s izračunatim intenzitetom u ovisnosti o temperaturi. Drugi postupak koristi spektralnu liniju bez reverzije, a temelji se na Kirchhoffovom zakonu, mjerenju apsorpcije tehnikom dvostrukog prolaza i upotrebom Abelove transformacije. Točni podaci o konstantama širenja i vjerojatnostima prijelaza nisu nužni.